PRINCETON UNIVERSITY

DEPARTMENT OF

AEROSPACE AND MECHANICAL SCIENCES

EROSION OF GRAPHITE SURFACE EXPOSED
TO HOT SUPERSONIC HYDROGEN GAS

by

Om P. Sharma

AMS Report No. 1038

Acknowledgements

Abstract

A theoretical model based on laminar boundary layer
flow equations is developed to predict the erosion rate
of a graphite (AGCarb-101) surface exposed to a hot super-
sonic stream of hydrogen gas. The supersonic flow in the
nozzle outside the boundary layer formed over the surface
of the specimen is determined by assuming one-dimensional
isentropic conditions. An overall surface reaction rate
expression based on the experimental studies by Clarke
and Fox is used to describe the interaction of hydrogen
with graphite. A satisfactory agreement is found between
the results of the computation, and the available experi-
mental data. Some shortcomings of the model, and further
possible improvements are discussed.

Table of Contents

Introduction

In order to achieve performance beyond that attainable by the best chemical rocket, the nuclear reactor has been applied to a rocket propulsion system. Over the past decade, considerable progress has been acheived in this direction, and the so-called NERVA (Nuclear Engine for Rocket Vehicle Application) propulsion system has received considerable development effort. Currently the feasibility of a similar, but smaller nuclear rocket engine is being explored. The NERVA flight engine has a nozzle extension after the regeneratively cooled nozzle,[1] and the nozzle extension is made of a graphite composite (AGCarb-101) material having the necessary structural strength as well as low secondary radiation qualities to reduce shielding requirements. A subscale experimental study was conducted in order to obtain the erosion rates of graphite composites when exposed to supersonic hydrogen atmosphere.[2] We have developed a theoretical model based on laminar boundary layer flow equations to predict these erosion rates.

Some details of the experimental setup can be found in Reference 2. The continuous supply of high pressure, hot hydrogen gas was obtained by using a one megawatt

plasma arc generator. The NERVA engine conditions were simulated by letting the gas expand through a specially designed water-cooled conical nozzle, and placing the specimen at a fixed position downstream of the throat. The duration for each test varied from half an hour to one hour. The heat and mass transfer as well as the chemical reaction take place within the boundary layer region over the surface of the specimen, and result in the erosion of the specimen. Due to the small magnitude of the observed erosion rates,[2] it is reasonable to treat the boundary layer flow as steady. Furthermore, for preliminary analysis, the flow will be considered laminar, and the presence of any dissociated component of the gas in the chamber will not be included. The kinetic data dealing with the reaction of a graphite composite (AGCarb-101) with hydrogen is not available. Therefore, the measurements of the reaction rate of a graphite filament with hydrogen by Clarke and Fox[3] are incorporated in this model. It was concluded by these authors that the reaction is a surface reaction below 3000°K. The flow outside the boundary layer is determined by assuming one-dimensional isentropic conditions. The details are described in the following sections.

Governing Equations

Assuming Fick's law of binary diffusion, the steady-state axi-symmetric laminar boundary layer flow for a

gaseous mixture is described by the following set of equations[4]

Mass conservation:

$$\frac{\partial(\rho u r)}{\partial x} + \frac{\partial(\rho v r)}{\partial y} = 0 \tag{1}$$

Momentum conservation:

$$\rho u \left(\frac{\partial u}{\partial x}\right) + \rho v \left(\frac{\partial u}{\partial y}\right) = -\left(\frac{dp}{dx}\right) + \frac{\partial}{\partial y}\left(\mu \frac{\partial u}{\partial y}\right) \tag{2}$$

Energy conservation:

$$\rho\left(\sum_i c_{p,i} Y_i\right)\left(u \frac{\partial T}{\partial x} + v \frac{\partial T}{\partial y}\right) = u\left(\frac{dp}{dx}\right) + \mu\left(\frac{\partial u}{\partial y}\right)^2$$

$$+ \frac{\partial}{\partial y}\left(k \frac{\partial T}{\partial y}\right) + \rho D\left(\sum_i c_{p,i} \frac{\partial Y_i}{\partial y}\right)\left(\frac{\partial T}{\partial y}\right) \tag{3}$$

Species conservation:

$$\rho u \left(\frac{\partial Y_i}{\partial x}\right) + \rho v \left(\frac{\partial Y_i}{\partial y}\right) = \frac{\partial}{\partial y}\left(\rho D \frac{\partial Y_i}{\partial y}\right) \tag{4}$$

In addition, we use the ideal gas equation of state for the mixture, that is,

$$p = \rho R^\circ T \left(\sum_i \frac{Y_i}{W_i}\right) \tag{5}$$

The pressure distribution in the boundary layer is determined from the non-viscous flow outside the boundary layer, and under the assumption of one-dimensional flow in the nozzle, is given by

$$-\left(\frac{dp}{dx}\right) = \rho_e u_e \left(\frac{du_e}{dx}\right) \tag{6}$$

We are thus dealing here with essentially five unknowns; namely, ρ, u, v, T, and Y_i, satisfying five equations (Eqs. (1) to (5)). A schematic representation of the distance coordinates (x,y) and r as well as the velocity components (u, v) is shown in Figure 1.

The velocity, temperature, and species mass fractions are subject to the following boundary conditions.

At $y = 0$ (eroding surface):

$$u = 0 \tag{7}$$

$$v \equiv v_w = (\dot{\omega}_{c,w}/\rho_w) \tag{8}$$

$$k_w \left(\frac{\partial T}{\partial y}\right)_w - \sum_i h_{i,w} \dot{\omega}_{i,w} = \left[k_s \left(\frac{\partial T_s}{\partial y}\right)\right]_{w^-} \tag{9}$$

$$\dot{\omega}_{i,w} = -\rho_w D_w \left(\frac{\partial Y_i}{\partial y}\right)_w + \dot{\omega}_{c,w} Y_{i,w} \tag{10}$$

At $y = \infty$ (boundary layer edge):

$$u = u_e \tag{11}$$

$$T = T_e \tag{12}$$

$$Y_{H_2} = 1, \text{ and } Y_i = 0, \; i \neq H_2 \tag{13}$$

The subscript w^- refers to the conditions interior of the specimen(s). The initial conditions as well as the detailed expressions for the transport parameters (μ, $c_{p,i}$, k, D) are discussed later.

From the experimental work of Clarke and Fox,[3] it is reasonable to conclude that the dominant product in the surface reaction of hydrogen with graphite in the temperature

and pressure range of interest is the methane gas. Then, it is necessary to solve only one species conservation equation, say for Y_{H_2}, since the following identity holds good in the mixture,

$$Y_{H_2} + Y_{CH_4} = 1 \qquad (14)$$

Since it is convenient to deal with the 'locally simi-lar' form of the boundary layer equations, we introduce new independent variables by combining the Levy and Mangler transformations and the Howarth-Dorodnitzyn transformation.[4] Let

$$s = \int_0^x (\rho_e \mu_e u_e r^2) \, dx' \qquad [gm^2 \ sec^{-2}] \qquad (15)$$

and

$$\eta = \left(\frac{u_e r}{\sqrt{2s}}\right) \int_0^Y \rho \, dy' \qquad [dimensionless] \qquad (16)$$

We also define non-dimensional x-component of velocity (U), temperature (θ), and a modified transverse velocity (V) as given below

$$U = (u/u_e) \qquad (17)$$

$$\theta = (T/T_e) \qquad (18)$$

$$V = \left(\frac{\sqrt{2s}}{\rho_e \mu_e u_e r}\right) \cdot \left[(\rho v) + \left(\frac{\sqrt{2s}}{r}\right)\left(\frac{\partial \eta}{\partial x}\right) U \right] \qquad (19)$$

In terms of the new variables defined by Eqs. (15) to (19), the governing Eqs. (1) to (4) become

$$\left(\frac{\partial V}{\partial \eta}\right) + U = -2s \left(\frac{\partial U}{\partial s}\right) \qquad (20)$$

$$\frac{\partial}{\partial \eta}\left(C \frac{\partial U}{\partial \eta}\right) - V\left(\frac{\partial U}{\partial \eta}\right) + \beta(s)\left[W_{H_2}\left(\overset{2}{\underset{i=1}{\Sigma}} \frac{Y_i}{W_i}\right) \cdot \theta - U^2\right]$$

$$= 2s\, U\left(\frac{\partial U}{\partial s}\right) \qquad (21)$$

$$\frac{\partial}{\partial \eta}\left(\frac{C \underset{i}{\Sigma} c_{p,i} Y_i}{Pr} \cdot \frac{\partial \theta}{\partial \eta}\right) - \left[(\underset{i}{\Sigma} c_{p,i} Y_i) V - \left(\frac{C}{Sc}\right)\left(\underset{i}{\Sigma} c_{p,i} \frac{\partial Y_i}{\partial \eta}\right)\right]\left(\frac{\partial \theta}{\partial \eta}\right)$$

$$= 2s\, (\underset{i}{\Sigma} c_{p,i} Y_i) U\left(\frac{\partial \theta}{\partial s}\right) + (\underset{i}{\Sigma} c_{p,i} Y_i)\, U\theta\Gamma(s)$$

$$+ \left(\frac{u_e^2}{T_e}\right)\left[W_{H_2}\left(\underset{i}{\Sigma} \frac{Y_i}{W_i}\right) \beta(s)\, U\theta - C\left(\frac{\partial U}{\partial \eta}\right)^2\right] \qquad (22)$$

$$\frac{\partial}{\partial \eta}\left(\frac{C}{Sc} \frac{\partial Y_{H2}}{\partial \eta}\right) - V\left(\frac{\partial Y_{H2}}{\partial \eta}\right) = 2s\, U\left(\frac{\partial Y_{H2}}{\partial s}\right) \qquad (23)$$

The boundary conditions stated in Eqs. (7) to (13) transform into the following forms:

At $\eta = 0$ (eroding surface):

$$U = 0 \qquad (24)$$

$$V_w = \left(\frac{\sqrt{2s}}{\rho_e \mu_e u_e r}\right) \cdot \dot{\omega}_{c,w} \qquad (25)$$

$$\left[\frac{\rho_w k_w u_e T_e r}{\sqrt{2s}}\right]\left(\frac{\partial \theta}{\partial \eta}\right)_w - \overset{2}{\underset{i=1}{\Sigma}} h_{i,w}\, \dot{\omega}_{i,w} = \left[k_s\left(\frac{\partial T_s}{\partial y}\right)\right]_{w^-} \qquad (26)$$

$$\dot{\omega}_{H_2,w} = -\left(\frac{\rho_w^2 D_w u_e r}{\sqrt{2s}}\right) \cdot \left(\frac{\partial Y_{H2}}{\partial \eta}\right)_w + \dot{\omega}_{c,w}\, Y_{i,w} \qquad (27)$$

At $\eta = \infty$ (edge of the boundary layer):

$$U = 1 \qquad (28)$$

$$\theta = 1 \qquad (29)$$

$$Y_{H_2} = 1, \text{ and } Y_i = 0, \; i \neq H_2 \qquad (30)$$

Note that the energy boundary condition at the eroding surface requires a solution of the heat transfer problem within the specimen. Except for the unexposed end portions, where the heat loss became important, the back surface of the specimen was heated by an ATJ graphite heating element in the experiments conducted for the determination of the erosion rates at Aerojet Nuclear Systems Company.[2] A realistic treatment of heat transfer within the specimen for this situation is too complex, and will also involve some unknown parameters. It is, therefore, proposed to assume a known constant value of the surface temperature (θ_w) which replaces the boundary condition stated in Eq. (26). Thus,

$$\theta(s,0) = \theta_w \tag{31}$$

The agreement between the theoretical and the experimental results will be improved by making different choices of θ_w.

External Flow

The flow outside the boundary layer over the specimen is dependent on the chamber conditions as well as the nozzle characteristics. The slight amount of dissociation present at the chamber conditions will be neglected. It is reasonable to treat the flow in the slender nozzle as one dimensional. Since there occurs a significant change in temperature along the nozzle, the variation in γ due to temperature cannot be completely ignored. To simplify the calculations, we will use two constant average values of γ such

that one of them (γ_I) is applicable for the region starting from the chamber to the leading edge of the specimen while the other $(\overline{\gamma})$ is for the flow over the specimen.

Therefore, for steady, one-dimensional and isentropic conditions, the velocity field in the flow external to the boundary layer over the specimen surface can be determined from the following differential equation,

$$\left(\frac{du_e}{dx}\right) = \frac{2\,u_e\,\sin\alpha\cdot\left(\dfrac{\overline{\gamma}p_o}{\rho_o}\right)\cdot\left[\dfrac{(\rho_o\,u_o\,r_o{}^2)^{\overline{\gamma}-1}}{(r_o+x\,\sin\alpha)^{2\overline{\gamma}-1}}\right]}{u_e{}^{\overline{\gamma}}+1-\left(\dfrac{\overline{\gamma}p_o}{\rho_o}\right)\cdot\left[\dfrac{(\rho_o\,u_o\,r_o{}^2)^{\overline{\gamma}-1}}{(r_o+x\,\sin\alpha)^{2\overline{\gamma}-2}}\right]} \tag{32}$$

In terms of the boundary layer variable s, defined in Eq. (15), we can show that

$$\beta(s) = \left(\frac{2s}{\rho_e\,\mu_e\,u_e\,r^2\,L}\right)\cdot\left(\frac{du_e}{d\overline{x}}\right) \tag{33}$$

and

$$\Gamma(s) = -\left[\frac{(\overline{\gamma}-1)\,u_e{}^2\,\rho_o}{\overline{\gamma}\,p_o}\right]\cdot\left(\frac{\rho_o}{\rho_e}\right)^{\overline{\gamma}-1}\cdot\beta(s) \tag{34}$$

The density (ρ_e) in the external stream will be obtained by making use of the mass conservation, that is,

$$\rho_e = (\rho_o\,u_o\,r_o{}^2)/(u_e\,r^2) \tag{35}$$

The pressure (p_e), and the temperature (T_e) can be calculated from the isentropic conditions given below,

$$\left(\frac{p_e}{p_o}\right) = \left(\frac{\rho_e}{\rho_o}\right)^{\overline{\gamma}} = \left(\frac{T_e}{T_o}\right)^{\left(\frac{\overline{\gamma}}{\overline{\gamma}-1}\right)} \tag{36}$$

Note that

$$r = r_o + x \sin \alpha = r_o + \bar{x} L \sin \alpha \tag{37}$$

The only other variable of interest in the external stream is the coefficient of viscosity for pure hydrogen gas (μ_e), [see Eq. (15)], which will be evaluated as a function of temperature (T_e) as described in the next section.

Transport Properties

The temperature dependences of the specific heats at constant pressure for hydrogen (c_{p,H_2}), and methane (c_{p,cH_4}) gases were described by the expressions given in McBride et al.[5] The coefficients of viscosity, and thermal conductivity for hydrogen and methane gases were calculated from the expressions based on kinetic theory, and the properties of the mixture were then determined by making use of the empirical equations.[6] Similarly, the binary diffusion coefficient (D) was calculated by using the kinetic theory expression quoted in the previously cited reference. The effect of the collision integral parameters appearing in the various transport coefficients, $\Omega_{12}^{(1,1)*}$ and $\Omega_i^{(2,2)*}$, was also included by approximating their temperature dependences by different analytical expressions valid over suitable ranges of temperature. The empirical expressions obtained in this manner were always within 2 - 3% of the values obtained from the "true" curves. It must, however, be noted that, due to the very small rate of erosion observed in the experiments, the mixture will consist of mostly hydrogen gas,

and, therefore, the transport coefficients will be insensitive to the mixture composition but will nevertheless be functions of temperature.

Chemical Kinetics

Clarke and Fox[3] concluded on the basis of their experimental studies that below 3000°K the reaction of graphite and hydrogen between 0.01 and 1.0 atm was a surface reaction whose rate was proportional to the hydrogen pressure and the square root of the dissociation constant of hydrogen. An empirical equation for the reaction rate, obtained by them and found to be in reasonable agreement with observed values, can be expressed as follows:

$$\dot{\omega}_{c,w} = \left(\frac{W_C}{W_{H_2}}\right)\left(\sum_i \frac{Y_i}{W_i}\right)^{-1} k_{SR} \ Y_{H_2,W} \ p_W \ \sqrt{k_D} \tag{38}$$

where $k_{SR} = 1 \cdot 20 \times 10^{-4}$ moles of carbon $cm^{-2} \ sec^{-1} \ (atms)^{-3/2}$, and k_D, the dissociation constant, is given by

$$k_D = A_D \ exp \ (- E_D/R°T_W) \tag{39}$$

with $A_D = 1 \cdot 947 \times 10^6$ atm, and $E_D = 1 \cdot 086 \times 10^5$ cal mole^{-1}. Note that Clarke and Fox assume in their analysis of the experimental data that chemical equilibrium exists at the surface of the specimen. In view of the assumption of a single step overall reaction,

$$C(s) + 2H_2 \rightarrow CH_4 \tag{40}$$

we have the following relationship

$$\dot{\omega}_{H_2,w} = (2W_{H_2}/W_c) \cdot \dot{\omega}_{c,w} \tag{41}$$

The mathematical formulation of the model is now complete, and a numerical solution is obtained as described in the next section.

Method of Solution

We are dealing here essentially with a set of non-linear coupled parabolic partial differential equations. A numerical scheme used previously by Sharma and Sirignano[7] for a similar system of equations has also been adopted in this particular case. We will describe below only some of the new features involved in the present problem.

The flow outside the boundary layer is governed by a nonlinear ordinary differential equation, Eq. (32), and was solved by using fourth-order Runge-Kutta method.[8] The initial condition, $u_e(x=0)$, was determined by assuming one dimensional isentropic flow in the nozzle, and by using a value of γ_{H_2} which resulted in giving the pressure at the leading edge of the specimen (p_o) equal to that obtained by extrapolating the experimentally observed values. γ_{H_2} obtained in this manner was always within $1\frac{1}{2}\%$ to a simple average of the γ_{H_2}-values corresponding to the chamber conditions and to those commonly existing at the downstream end of the specimen. A second constant average value of

γ_{H_2}, which corresponded more closely to the temperature variations in the domain of the specimen, was used in Eq. (32), and was not changed from one test condition to another. These choices of γ_{H_2} led to the pressure profiles in the domain of its specimen within 1% of the more elaborate two-dimensional, non-equilibrium calculations due to Hamann.[9] Thus, $u_e(\overline{x})$ was obtained along the specimen at stations separated by a uniform step size of $D\overline{x} = 0.01$. The other flow variables like ρ_e, p_e, T_e, etc. were then obtained by using Eqs. (35) and (36).

The initial conditions for the governing boundary layer equations, Eqs. (20) to (23), were assumed to be given by a locally similar solution of these equations at a small enough value of s. A choice of $\overline{x}_i = 0.01$ was used and the results were found to be insensitive to any reasonable reductions in this value. The continuity equation, Eq. (20), having a first order derivative in η was directly integrated by using extended Simpson's rule.[8]

Note that the external flow field is determined at uniform intervals in $\overline{x}$ so that the corresponding values of s are no longer uniform, [see Eq. (15)]. Therefore, in order to obtain the difference-differential forms of Eqs. (20) to (23), we replace the s-derivatives by the difference expressions with the help of general Lagrange formula.[8]

That is,

$$\left(\frac{\partial U}{\partial s}\right)_{(i,j)}^{(k)} = \left[\frac{U_{(i,j)}^{(k)} - U_{(i-1,j)}}{s_i - s_{i-1}}\right] \tag{42}$$

for two-point approximation

and

$$\left(\frac{\partial U}{\partial s}\right)_{(i,j)}^{(k)} = \frac{(s_i - s_{i-2}) + (s_i - s_{i-1})}{(s_i - s_{i-2})(s_i - s_{i-1})} \cdot U_{(i,j)}^{(k)}$$

$$- \frac{(s_i - s_{i-2})}{(s_i - s_{i-1})(s_{i-1} - s_{i-2})} \cdot U_{(i-1,j)}$$

$$+ \frac{(s_i - s_{i-1})}{(s_i - s_{i-2})(s_{i-1} - s_{i-2})} \cdot U_{(i-2,j)} \tag{43}$$

for three-point approximation

Two-point approximation, Eq. (42), will be used only once in moving the first step away from the locally similar solution. The terms like $\frac{\partial}{\partial \eta}\left(c\frac{\partial U}{\partial \eta}\right)$ are expanded into $\left\{c\left(\frac{\partial^2 U}{\partial \eta^2}\right) + \left(\frac{\partial c}{\partial \eta}\right)\left(\frac{\partial U}{\partial \eta}\right)\right\}$ before expressing them in the finite difference approximations. All η-derivatives were replaced by central difference formulae. The various transport parameters like C, Pr, Sc, etc. were determined from the results of the previous iteration. The linearization and iteration procedure was done in the same manner as described by Sharma and Sirignano.[7]

The step size in η-direction was kept fixed at 0.05, while that in $\bar{x}$-direction varied from 0.05 for the first two stations to 0.10 till the end of the specimen. The

external flow conditions were found to be adequately satis-
fied at η_{max} = 7.00. The iteration cycle was stopped when
a prescribed convergence of 1 in 10^4 was achieved for tem-
perature values of successive iterations.

Results and Discussion

The detailed measurements in each test run of Refer-
ence 2 consisted of the erosion rates, and the pressures
at four locations along the specimen. In the present cal-
culations, we obtain, in addition to the erosion rates and
pressures, the detailed profiles of the x-component of ve-
locity, temperature, and the species mass fractions as
well as the rate of heat transfer at the specimen surface.
Since the surface temperature of the specimen is not known
a priori, a couple of trial runs are necessary to obtain
a value of surface temperature which gives erosion rates
close to the experimental points.

The magnitudes of the various physical quantities in-
volved in the computation are listed next. r_t = 0.3175 cm,
α = 7°, r_o = 0.5144 cm, L = 3.95 cm, $\overline{\gamma}$ = 1.385, W_{H_2} = 2.016
gm mole^{-1}, W_C = 12.011 gm mole^{-1}, and W_{CH_4} = 16.043 gm mole^{-1}.
In order to transform the mass burning rate (gm cm^{-2} sec^{-1})
into the measured erosion rate (cm sec^{-1}), we made use of
the density of the AGCarb-101, that is, ρ_C = 1.45 gm cm^{-3},
as determined at the Aerojet Nuclear Systems Company[10].

The results of the solution of Eqs. (20 to (23) for
the stagnation conditions of test run No. W-110 of Reference 2

are plotted in Figs. 2 to 6 when T_W = 2188°K. The agreement between the calculated and the measured pressure (see Fig. 2) is quite good, and the differences at various locations ramain within a few percent. Note that an accurate determination of p is very important since the erosion rate is directly proportional to p [see Eq. (38)]. The general features of the velocity (Fig. 3) and the temperature (Fig. 4) profiles are similar to those commonly observed in other boundary layer flows. A plot of $q_w[= k_w(\partial T/\partial y)_w]$ vs $\bar{x}$ in Fig. 5 shows that the heat is always being transferred from the gaseous phase to the specimen. Note that q_w is dependent on a choice for the initial value of $\bar{x}$, and that the effect is insignificant towards the downstream portion of the specimen. A choice of $\bar{x}$ = 0.01 was found quite adequate for the present computations because it had avoided the singularity at $\bar{x}$ = 0 as well as was reasonably small enough not to give results in appreciable error. The erosion rates were, however, insensitive to the value of $\bar{x}_i$ as long as we dealt with constant surface temperature conditions. Fig. 6 contains the comparison between the calculated erosion rates, and the experimental points. In view of some complexities involved in the experimental setup as well as the simplifications made in the present model, the agreement between the two results is considered quite satisfactory. It must be pointed out here that this comparison varies from one test run condition to another without any discernible pattern. Furthermore, since the experimental points for

different test runs having similar stagnation conditions do not indicate similar functional dependences, there is a possibility of some errors in the measurements which have not been estimated.

The amount of hydrogen gas consumed during the erosion process was found to be extremely small; $Y_{H_2,w}$ being generally of the order of 0.999. Thus, no detailed profiles for the species mass fractions were plotted. More importantly, the erosion rates can thus be calculated directly from Eq. (39) by setting $Y_{H_2,w}$ equal to unity, and by using the values of p_w obtained from a solution of equations governing the external flow. Of course, the boundary layer equations must be solved if the heat transfer rates are to be determined as well as if the surface temperature is to be determined by solving the coupled heat transfer problem within the specimen.

The general features of the detailed profiles computed for other test conditions are very similar to those of the previous case except that q_w becomes negative for test conditions in which the (assumed) surface temperature is higher than the stagnation value. Some of the computed erosion rates for different test conditions are shown in Fig. 7. The agreement between the calculated curves and the experimental points is thus extremely good in tests like W-111, W-112, and W-115, while there is an appreciable error for test conditions of W-142. Further improvements in the theoretical model are possible as well as some

realistic error estimates of the measured quantities are necessary.

Conclusions

The agreement between the theoretical curves and the experimental points is quite reasonable, considering the fact that the surface boundary condition for the tempera- ture (or the energy) equation in the actual experiments is far more complicated than the one used in the present cal- culations. The general trend of the curves is also simi- lar to those of the experimental points. The surface re- action model, therefore, would appear adequate in the pre- diction of erosion rates for specimen surface temperatures less than $3000^{\circ}K$. Further improvements in the model can be achieved by including the dissociation and the turbu- lent flow effects as well as the coupled heat transfer problem within the specimen. In addition, for a precise agreement between theory and experiment, experiments with simplified energy boundary conditions, like constant sur- face temperature, must be performed.

References

[1]Altseimer, J. H., Mader, G. F., and Stewart, J. J., "Operating Characteristics and Requirements for the NERVA Flight Engine," AIAA Paper No. 70-676, June 1970, pp. 1-9.

[2]Inouye, H. H., Claassen, L. B., and Shurley, L. A., "Final Test Report: AGCarb-101 Corrosion/Erosion Evaluation Program," 7750:R0834, April 1970, Aerojet Nuclear Systems Company, Sacramento, Calif.

[3]Clarke, J. T. and Fox, B. R., "Reaction of Graphite Filaments with Hydrogen above 2000°K, "The Journal of Chem. Phys., Vol. 46, No. 3, Feb. 1967, pp. 827-836.

[4]Lees, L., "Laminar Heat Transfer over Blunt-Nosed Bodies at Hypersonic Flight Speeds," Jet Propulsion, Vol. 26, No. 4, April 1956, pp. 259-269.

[5]McBride, B. J., Heimel, S., Ehlers, J. G., and Gorden, S., "Thermodynamic Properties to 6000°K for 210 Substances Involving the First 18 Elements," NASA SP-3001, March 1963.

[6]Penner, S. S., "Chemistry Problems in Jet Propulsion," MacMillan, New York, 1957, pp. 245-250.

[7]Sharma, O. P. and Sirignano, W. A., "On the Ignition of a Pre-Mixed Fuel by a Hot Projectile," Comb. Sc. and Tech., Vol. 1, No. 6, May 1970, pp. 481-494.

[8]Abramowitz, M. and Stegun, I. A., ed., "Handbook of Mathematical Functions with Formulas, Graphs, and Mathematical Tables," NBS AMS 55, March 1965, p. 896, p. 886, pp. 882-884.

[9]Hamann, R. J., private communication, Guggenheim Laboratories, Princeton University, Princeton, New Jersey.

[10]David, H. O., Kotfila, R. J., and Schleicher, W. J., "The Fabrication and Properties of the Fibrous Reinforced Graphite Composite, AGCarb-101," RN-S-0549, March 1970, Aerojet Nuclear Systems Company, Sacramento, California.

Nomenclature

A_D = a known constant [see Eq. (39)] (atm)

$c_{p,i}$ = specific heat at constant pressure of species i
$(cal\ gm^{-1} {}^\circ K^{-1})$

C = $(\rho\mu/\rho_e\mu_e)$

D = binary diffusion coefficient $(cm^2\ sec^{-1})$

E_D = a known constant [see Eq. (39)] $(cal\ mole^{-1})$

h_i = specific enthalpy of species i $[\int_{T_r}^{T} c_{p,i}\ dT + h_i^r]\ (cal\ gm^{-1})$

k = thermal conductivity $(cal\ cm^{-1} sec^{-1} {}^\circ K^{-1})$

k_D = dissociation constant [see Eq. (39)] (atm)

k_{SR} = known constant [see Eq. (38)] (moles of carbon $cm^{-2} sec^{-1}$ $(atm)^{-3/2}$)

L = length of the graphite specimen (cm)

p = pressure (atm)

Pr = Prandtl number $[= \mu(\sum_i c_{pi} Y_i)/k]$

q = heat flux $[= k(\partial T/\partial y)]\ (cal\ cm^{-2} sec^{-1})$

r = perpendicular distance of the specimen surface from the axis of symmetry (cm)

r_o = radius of the nozzle at the leading edge of the graphite specimen (cm)

r_t = radius of the nozzle throat (cm)

R^O = universal gas constant $(cal\ mole^{-1} {}^\circ K^{-1})$

s = modified coordinate in x-direction [see Eq. (15)] $(gm^2 sec^{-2})$

Sc = Schmidt number $[= (\mu/\rho D)]$

T = temperature $(^\circ K)$

u $\quad$ = x-component of velocity (cm sec^{-1})

U $\quad$ = non-dimensional velocity [see Eq. (17)]

v $\quad$ = y-component of velocity (cm sec^{-1})

V $\quad$ = modified transverse velocity [see Eq. (19)]

W_i $\quad$ = molecular weight of species i (gm mole^{-1})

x $\quad$ = distance along the specimen surface (cm)

$\bar{x}$ $\quad$ = non-dimensional distance [=(x/L)]

y $\quad$ = distance perpendicular to the specimen surface (cm)

Y_i $\quad$ = mass fraction of species i

α $\quad$ = half angle of the divergent part of the nozzle [= 7°]

β $\quad$ = $(2s/u_e)(du_e/ds)$

γ $\quad$ = ratio of the specific heats at constant pressure
$\qquad$ and at constant volume

Γ $\quad$ = $(2s/T_e)(dT_e/ds)$

η $\quad$ = transverse coordinate [see Eq. (16)]

θ $\quad$ = dimensionless temperature [see Eq. (18)]

μ $\quad$ = coefficient of viscosity (gm cm^{-1}sec^{-1})

ρ $\quad$ = density (gm cm^{-3})

$\dot{\omega}_i$ $\quad$ = reaction rate of species i (gm cm^{-2}sec^{-1})

Subscripts

c $\quad$ = carbon

e $\quad$ = external flow (y = ∞)

i $\quad$ = species (H_2 and CH_4) or a mesh point in s-direction

j $\quad$ = a mesh point in η-direction

o $\quad$ = leading edge of the specimen (x = 0)

r   = reference state

s   = specimen

w   = specimen surface $(y = 0)$

Superscripts

-       = non-dimensional or average

k   = iteration number

List of Figures

Specimen

u_e

(x,u)

(y,v)

r

Boundary layer edges

Fig.1(Sharma)

Fig. 2 (Sharma)

Test no. W-110
$T_w = 2188°K$

Curve	(x/L)	u_e(cm sec^{-1})
I	0.01	6.3237×10^5
II	0.41	7.0021×10^5
III	0.91	7.4226×10^5

Fig. 3 (Sharma)

Test no. W-110
$T_c = 2506°K$
$T_w = 2188°K$

Curve	(x/L)	T_e(°K)
I	0.01	1239.4
II	0.41	934.7
III	0.91	730.4

Fig. 4 (Sharma)

Fig.5(Sharma)

Test no. W-IIO
$T_c = 2506°K$
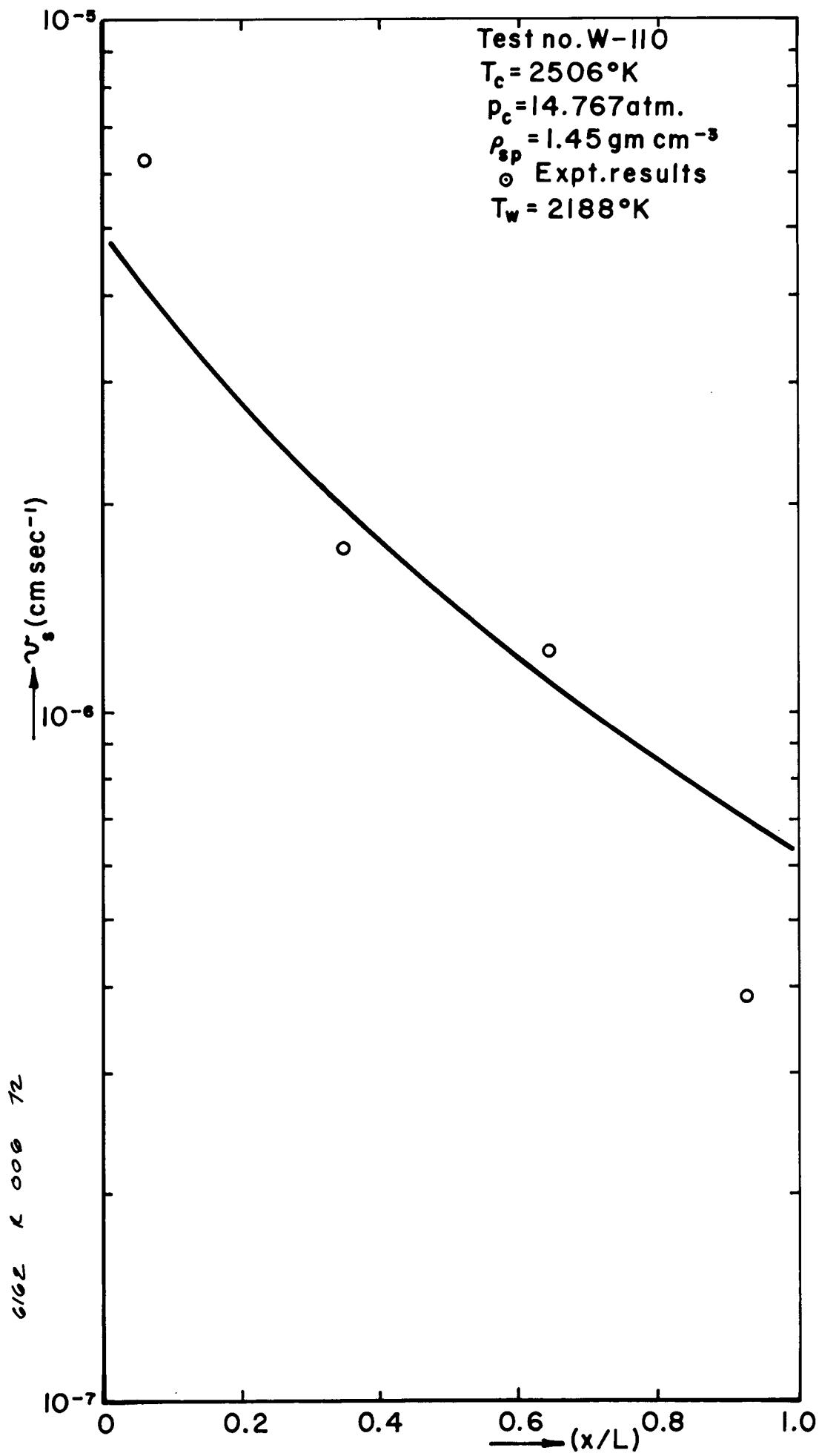$p_c = 14.767$ atm.
$\rho_{sp} = 1.45$ gm cm^{-3}
⊙ Expt. results
$T_w = 2188°K$

Fig. 6 (Sharma)

Fig.7 (Sharma)